

# Ultrasensitive detection of DNA by the PCR-Induced generation of DNazymes: The DNazyme primer approach†

Zoya Cheglakov, Yossi Weizmann, Moritz K. Beissenhirtz and Itamar Willner\*

Received (in Cambridge, UK) 11th April 2006, Accepted 1st June 2006

First published as an Advance Article on the web 26th June 2006

DOI: 10.1039/b605205c

The ultrasensitive detection of DNA is achieved by PCR-induced evolution of a DNazyme.

Amplification is a fundamental element of bioanalysis. Enzymes,<sup>1–3</sup> DNazymes,<sup>4,5</sup> nanoparticles<sup>6–8</sup> and nano-scale force interactions<sup>9</sup> are widely used for the sensitive detection of biorecognition events. Within this area, amplified analysis of DNA is particularly challenging, since it can provide an effective means to detect pathogens, analyze genetic disorders, and be used for forensic applications.

There is a continuous impetus to improve the polymerase chain reaction (PCR) process by providing fast and reliable methods for *in situ* monitoring and quantification of the analyte nucleic acids. Ingenious approaches that apply tailored photonically active primers<sup>10</sup> or DNazyme units<sup>11</sup> have been reported. The QZyme technology<sup>11</sup> includes the complementary sequence to DNazyme as part of a primer, and its replication leads to the DNazyme. The resulting DNazyme triggers the cleavage of an internally-quenched donor–acceptor oligonucleotide that acts as a fluorescent reporter for DNA analysis. An alternative approach utilizes an internally-quenched hairpin nucleic acid tethered to the PCR primer. Upon the replication of the template and the subsequent opening of the hairpin loop, followed by hybridization to the product, a fluorescent scorpion-type structure is formed which acts as the reporter for DNA analysis.<sup>10</sup>

We report on a novel approach to monitor and quantify PCR products, using a DNazyme label that yields colorimetric or chemiluminescent readout signals. The novel method, an alternative to the Real-Time polymerase chain reaction (Real-Time PCR), is applied to detect ~40 molecules of M13 phage DNA in a sample of 50  $\mu$ l.

PCR provides a general protocol for amplified detection of DNA, and Real-Time PCR allows quantification of analyte nucleic acids. In Real-Time PCR fluorescent-labeled primers or intramolecular quenched “hairpin” primers, that are “lightened-up” upon the PCR process, are commonly used as active labels for the PCR process.<sup>12–15</sup> Besides the high cost of the modified primers, the sensitivity of the method is controlled only by the PCR. The specific DNazyme employed in our study is a nucleic acid G-quadruplex structure that binds hemin to yield a complex that mimics peroxidase activities.<sup>16,17</sup> The DNazyme catalyzes the

oxidation of 2,2'-azino-bis(3-ethylbenzothiazoline-6-sulfonic acid), ABTS<sup>2-</sup>, by H<sub>2</sub>O<sub>2</sub>, to a green colored product or leads, in the presence of H<sub>2</sub>O<sub>2</sub>/luminol, to the generation of chemiluminescence.<sup>18</sup>

The method for the amplified detection of the M13 phage DNA is depicted in Fig. 1. The primer 1 includes a nucleic acid segment (green) complementary to the M13 phage DNA analyte, and is linked by a nucleic acid sequence (light green) and an oxyethyleneglycol bridge (blocker, red) to the nucleic acid exhibiting the DNazyme sequence (light blue). The DNazyme sequence forms a hairpin structure with the other end of the primer, thus prohibiting the active DNazyme structure. The PCR cycle includes the replication of the double-strand between 1 and the analyte (target DNA) and the separation of the double-strand. Subsequently, the synthesized template is hybridized with the second primer 2 that includes a nucleic acid segment (black) complementary to the template, a sequence (light green) linked through the oxyethyleneglycol (blocker, red) tether to the

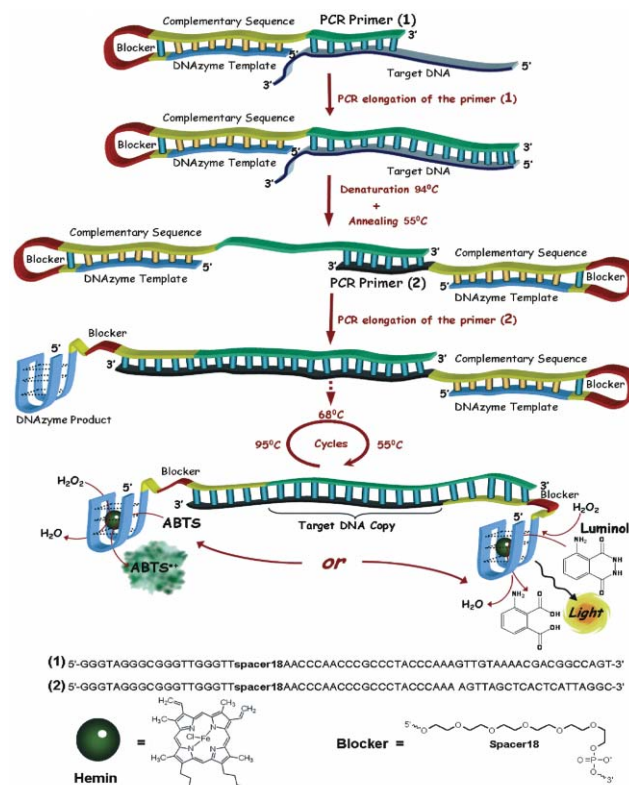


Fig. 1 Scheme for the amplified detection of DNA by the PCR replication of DNazyme-containing units and their analysis by colorimetric or chemiluminescence methods.

Institute of Chemistry and The Farkas Center for Light-Induced Processes, The Hebrew University of Jerusalem, 91904 Jerusalem, Israel. E-mail: willner@vms.huji.ac.il; Fax: +972 2 6527715; Tel: +972 2 6585272

† Electronic supplementary information (ESI) available: Full experimental protocols for PCR assay, colorimetric and chemiluminescence measurements. See DOI: 10.1039/b605205c

DNAzyme sequence (light blue). As before, the hairpin structure prohibits the generation of the G-quadruplex DNAzyme structure. Subsequent polymerization, in the presence of polymerase, replicates the template, and the process results in the zipping off of the hairpin structure. This leads to the formation of the G-quadruplex structure that, upon intercalation of hemin, yields the active DNAzyme. Thus, by the application of the two primers **1** and **2**, the respective nucleic acid templates are continuously generated by the appropriate replication/thermal cycles. Note that the polymerization of the respective templates is always terminated at the oxyethyleneglycol tethers (blocker). Thus, free single-stranded nucleic acid residues that yield, in the presence of hemin, the peroxidase-mimicking DNAzyme are generated.

Fig. 2 shows the time-dependent oxidation of  $\text{ABTS}^{2-}$  by  $\text{H}_2\text{O}_2$  catalyzed by the DNAzyme templates generated after 30 PCR cycles of 1.5 min, and using different concentrations of the analyte M13 phage DNA. As the concentration of the M13 phage DNA is higher, the oxidation of  $\text{ABTS}^{2-}$  is enhanced, implying a higher content of the active DNAzyme units. The system in its present composition reaches optimal DNAzyme activities at a concentration of M13 phage DNA, which corresponds to  $3 \times 10^{-12}$  M; and higher analyte concentrations have a minute effect on the rate of the  $\text{ABTS}^{2-}$  oxidation. This is due to the rapid consumption of the added nucleotide bases that yield similar amounts of the active DNAzyme. Fig. 2, inset, shows the visual colorimetric detection of different concentrations of the M13 phage DNA. Fig. 2 curve (f) shows the rate of  $\text{ABTS}^{2-}$  oxidation upon the application of the primers **1** and **2** to analyze the foreign *Calf Thymus* DNA,  $3 \times 10^{-12}$  M, and subjecting the system to the same number of thermal cycles used to analyze the M13 phage DNA. A minute rate of oxidation of  $\text{ABTS}^{2-}$  is observed. In fact, the same low rate of

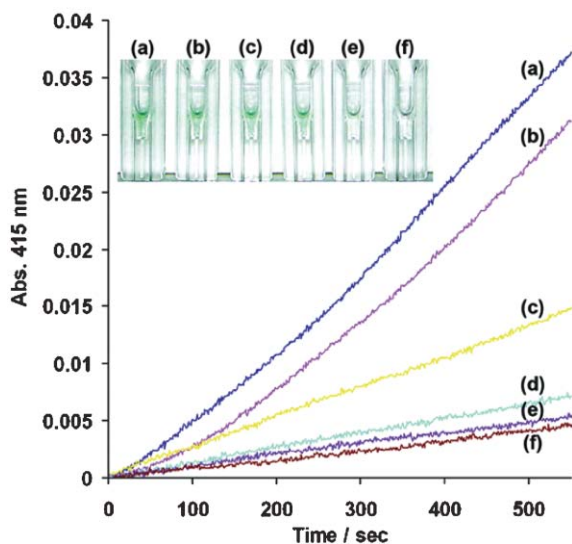


**Fig. 2** Time-dependent absorbance changes resulting from the oxidation of  $\text{ABTS}^{2-}$ ,  $1.82 \times 10^{-4}$  M, by  $\text{H}_2\text{O}_2$ ,  $4.4 \times 10^{-5}$  M, in the presence of hemin,  $4 \times 10^{-7}$  M, and the DNAzymes formed upon the analysis of M13 phage DNA: (a)  $3 \times 10^{-10}$  M (b)  $3 \times 10^{-12}$  M (c)  $3 \times 10^{-14}$  M (d)  $3 \times 10^{-16}$  M (e)  $3 \times 10^{-18}$  M (f) Analysis of the foreign *Calf Thymus* DNA  $3 \times 10^{-12}$  M. In all experiments 30 PCR cycles consisting of denaturation,  $94^\circ\text{C}$ , 30 s; annealing,  $55^\circ\text{C}$ , 30 s; polymerization,  $68^\circ\text{C}$ , 30 s, were employed. Inset: Images of the colored solutions generated by the replicated DNAzyme products upon analyzing the respective systems.

$\text{ABTS}^{2-}$  oxidation is observed upon the application of hemin only, or the foreign *Calf Thymus* DNA–hemin mixture itself as catalysts for the  $\text{H}_2\text{O}_2$ -mediated oxidation of  $\text{ABTS}^{2-}$ . Thus, the low intensity color signal, observed upon analyzing the foreign DNA may be attributed to the inefficient oxidation of  $\text{ABTS}^{2-}$  by free hemin. This low absorbance due to the oxidation of  $\text{ABTS}^{2-}$  by free hemin may be considered as the background color of the system. Taking into account the volume of the M13 phage DNA that is analyzed, the experimental detection limit translates to 90 molecules of analyte in the 50  $\mu\text{l}$  sample.

Fig. 3(A) depicts the results of a similar experiment using the DNAzyme-stimulated generation of chemiluminescence in the presence of  $\text{H}_2\text{O}_2$ –luminol. As the concentration of the analyte increases, the content of the PCR-induced replicated templates that include the G-quadruplex DNAzyme structures increases, and the biocatalytic generation of chemiluminescence by the DNAzyme–hemin complex is enhanced. In these experiments, we maintain the

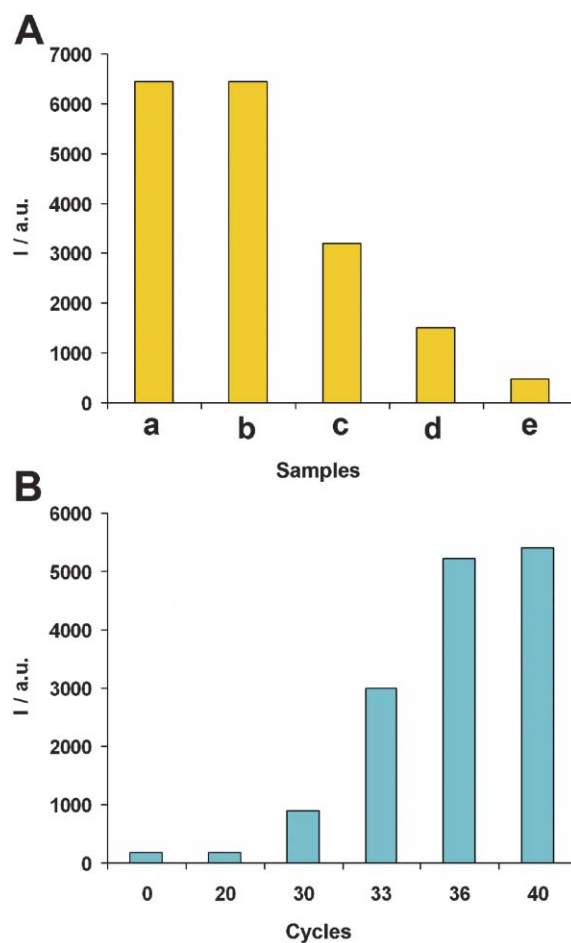


**Fig. 3** (A) Chemiluminescence intensities generated by the DNAzyme-labeled replicas formed upon analysis of M13 phage DNA: (a)  $1.2 \times 10^{-10}$  M (b)  $1.2 \times 10^{-12}$  M (c)  $1.2 \times 10^{-14}$  M (d)  $1.2 \times 10^{-18}$  M (e) Control experiment analyzing the foreign *Calf Thymus* DNA,  $1.2 \times 10^{-12}$  M. In all experiments hemin,  $1 \times 10^{-9}$  M,  $\text{H}_2\text{O}_2$ ,  $3 \times 10^{-2}$  M, and luminol,  $5 \times 10^{-4}$  M, are included in the analyzed reaction media. All experiments involved 30 PCR cycles, as described in the caption of Fig. 2. (B) Chemiluminescence intensities generated by systems analyzing M13 phage DNA,  $1.2 \times 10^{-18}$  M, and employing different numbers of PCR replication cycles.

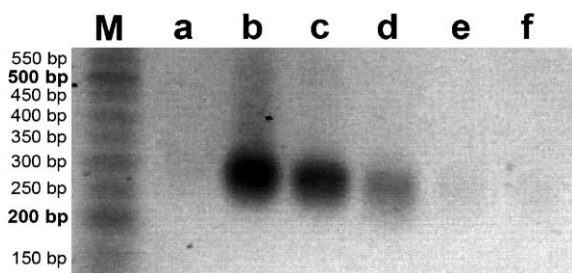


**Fig. 4** Agarose-gel electrophoresis of the DNAzyme-labeled replicated DNAs (30 replication cycles) formed upon the analysis of M13 phage DNA: (b)  $3 \times 10^{-10}$  M (c)  $3 \times 10^{-12}$  M (d)  $3 \times 10^{-14}$  M (e)  $3 \times 10^{-16}$  M (f)  $3 \times 10^{-18}$  M. Run (a) corresponds to the analysis of the control foreign *Calf Thymus* DNA,  $3 \times 10^{-12}$  M.

concentration of hemin at a low level, corresponding to  $1 \times 10^{-9}$  M, to generate a low intensity of chemiluminescence background generated by the hemin–luminol– $H_2O_2$  system itself. In fact, the chemiluminescence intensity levels-off at a concentration of M13 phage DNA which corresponds to  $1.2 \times 10^{-12}$  M. This originates from the fact that the hemin concentration is limited, and is fully consumed in generating the active DNAzyme at high concentrations of the analyte. It should be noted that the M13 phage DNA at a concentration of  $1.2 \times 10^{-18}$  M (that corresponds to  $\sim 36$  copies in the sample) is detected with a signal-to-background ratio corresponding to 4, upon analyzing the control sample of *Calf Thymus* DNA at a concentration of  $1.2 \times 10^{-12}$  M(!!!). The effect of the number of PCR cycles on the intensity of emitted chemiluminescence was examined too. Fig. 3(B) shows the intensity of the emitted chemiluminescence upon analyzing M13 phage DNA,  $1.2 \times 10^{-18}$  M, using a variable number of PCR cycles. A non-linear increase in the chemiluminescence intensity is observed, and after 36 PCR cycles, the emitted light intensity levels off to a constant saturated value. This is due to the consumption of hemin by its incorporation into the DNAzyme units. The reproducibility of the analytical procedure is very good, and within a set of eight experiments, analyzing  $3 \times 10^{-14}$  M of the M13 phage DNA, the color or chemiluminescent signals were within a range of  $\pm 4\%$ .

The replication of the DNAzyme-functionalized templates was confirmed by electrophoretic experiments. Fig. 4 shows the denaturing electrophoresis of the generated PCR products consisting of the labeled DNAzymes formed upon analyzing different concentrations of the viral DNA, while performing 30 PCR cycles. Runs (b) to (f) show the DNAzyme-labeled products (consisting of *ca.* 242 bp being replicated, tethered to a DNAzyme label composed of a single-stranded sequence of 23 bases). As the content of the analyzed DNA is higher, the intensity of the electrophoretic band is enhanced. The appropriate product-band is clearly visible upon the analysis of the M13 phage DNA at a concentration of  $3 \times 10^{-18}$  M. Run (a) shows the negative electrophoretic control experiment, where the *Calf Thymus* DNA,  $3 \times 10^{-12}$  M, is analyzed according to Fig. 1 using **1** and **2** as the primers. No band is formed in this system, indicating that no replication occurred.

In conclusion, the present study introduces a novel method to quantify PCR products. While the Real-Time PCR method allows the continuous analysis of the replication process, it suffers from fundamental limitations encountered with the expensively tailored primers and the need for expensive instrumentation. Our method introduces an alternative protocol that allows the time-dependent withdrawal of PCR samples and the quantitative analysis of the products by colorimetric or chemiluminescent reactions of the generated DNAzymes. The formation of the DNAzymes in our systems represents a further advantage, since the resulting catalysts amplify the recognition events by their colorimetric or chemiluminescence readout signals. We note, however, that the DNAzyme-mediated reactions used in our study employ  $H_2O_2$  as co-substrate. This ingredient is certainly a disadvantage, as it is not compatible with the PCR reaction, thus allowing the readout of the process only through the analysis of the final end-point product. The paradigm of the PCR replication of DNAzymes that act as effective catalytic reporter units may be extended to other DNAzymes. Although at this phase it is premature to assess the cost-effectiveness of the primers used in the present study and the internally-quenched reporters used in the other Real-Time PCR system, a rough estimation suggests that the cost of our primers is less than 50% of the price of currently available reporters. We believe that the method has broad applicability for rapid, easy, quantitative, and ultrasensitive, analysis of any DNA.

This research is supported by the Israel Ministry of Science as an Infrastructure Project.

## Notes and references

- 1 D. J. Caruana and A. Heller, *J. Am. Chem. Soc.*, 1999, **121**, 769–774.
- 2 F. Patolsky, A. Lichtenstein, M. Kotler and I. Willner, *Angew. Chem., Int. Ed.*, 2001, **40**, 2261–2265.
- 3 E. Hadas, L. Soussan, I. Rosen-Margalit, A. Farkash and J. Rishpon, *J. Immunoassay*, 1992, **13**, 231–252.
- 4 T. Niazov, V. Pavlov, Y. Xiao, R. Gill and I. Willner, *Nano Lett.*, 2004, **4**, 1683–1687.
- 5 Y. Xiao, V. Pavlov, T. Niazov, A. Dishon, M. Kotler and I. Willner, *J. Am. Chem. Soc.*, 2004, **126**, 7430–7431.
- 6 J. Wang, D. Xu, A.-N. Kawde and R. Polsky, *Anal. Chem.*, 2001, **73**, 5576–5581.
- 7 G. Liu, T. M. H. Lee and J. Wang, *J. Am. Chem. Soc.*, 2005, **127**, 38–39.
- 8 L. He, M. D. Musick, S. R. Nicewarner, F. G. Salinas, S. J. Benkovic, M. J. Natan and C. D. Keating, *J. Am. Chem. Soc.*, 2000, **122**, 9071–9077.
- 9 J. Fritz, M. K. Baller, H. P. Lang, H. Rothuizen, P. Vettiger, E. Meyer, H.-J. Güntherodt, Ch. Gerber and J. K. Gimzewski, *Science*, 2000, **288**, 316–318.
- 10 A. Solinas, L. J. Brown, C. McKeen, J. M. Mellor, J. Nicol, N. Thelwell and T. Brown, *Nucleic Acids Res.*, 2001, **29**, E96.
- 11 A. V. Todd, C. J. Fuery, H. L. Impey, T. L. Applegate and M. A. Haughton, *Clin. Chem.*, 2000, **46**, 625–630.
- 12 C. A. Heid, J. Stevens, K. J. Livak and P. M. Williams, *Genome Res.*, 1996, **6**, 986–994.
- 13 M. M. Mhlanga and L. Malmberg, *Methods*, 2001, **25**, 463–471.
- 14 J. A. Vet, B. J. Van der Rijt and H. J. Blom, *Expert Rev. Mol. Diagn.*, 2002, **2**, 77–86.
- 15 B. K. Saha, B. Tian and R. P. Bucy, *J. Virol. Methods*, 2001, **93**, 33–42.
- 16 P. Travascio, P. K. Witting, A. G. Mauk and D. Sen, *J. Am. Chem. Soc.*, 2001, **123**, 1337–1348.
- 17 D. J. F. Chinnapen and D. Sen, *Biochemistry*, 2002, **41**, 5202–5212.
- 18 V. Pavlov, Y. Xiao, R. Gill, A. Dishon, M. Kotler and I. Willner, *Anal. Chem.*, 2004, **76**, 2152–2156.